RF Complex Permittivity Characterization of ScAlN Thin Films

Aurelio Venditti
Politecnico di Torino
Turin, Italy

Luca Colombo, Pietro Simeoni, and Matteo Rinaldi
SMART Center, Northeastern University
Boston MA, USA

***Summary*—The present paper describes the application of a one-port non-resonant reflection measurement on a matrix of Metal-Insulator-Metal (MIM) test structures for the extraction of the dielectric constant and the loss tangent as a function of frequency (up to 10 GHz) of piezoelectric Aluminum Nitride (AlN) thin films with Scandium (Sc) doping of 15% and 28%. The obtained results demonstrate the dependence of these properties on the Sc doping concentration and, in particular, the linear increasing of the loss tangent as a function of the frequency. This analysis provides both preliminary results for the dielectric characterization of this novel material and useful insights for the design of ScAlN radio frequency (RF) piezoelectric resonators.**

Keywords—ScAlN; complex permittivity; resonators; MEMS

I. INTRODUCTION

The Internet of Things (IoT) and raise of 5G adoption demand a selection of devices that can cover an operational frequency range going from few MHz up to several GHz. To this aim, novel piezoelectric materials drew research interest in recent years to improve existing designs and achieve the required performance for radio frequency (RF) front-end components [1]. Among them, Scandium-doped Aluminum Nitride (ScAlN) has been found to significantly boost the piezoelectric coefficients of AlN. Several works from literature reported on the functional dependence of ScAlN from the Scandium (Sc) doping concentration [2], but, at the best of our knowledge, measurements on ScAlN dielectric properties as a function of frequency have not been already reported. Such investigation is necessary to improve the characterization of different ScAlN devices operating over a broad frequency range. Therefore, the present paper aims to fill this gap by performing dielectric characterization of AlN thin films with Sc doping of 15% and 28% by extracting their complex permittivity in terms of dielectric constants and loss tangents as a function of frequency up to 10 GHz. This type of characterization helps improving the matching between different devices at the system level, and it highlights their limitations due to intrinsic dielectric losses, since *ab initio* values found in literature can differ from the ones measured in fabricated devices due to processing non-idealities [3].

Various techniques can be used to measure the complex permittivity of dielectric materials [4], but all of them can be broadly divided into two categories, called resonant and non-resonant [5]. In this work, one-port non-resonant reflection measurements have been performed on a matrix of Metal-Insulator-Metal (MIM) test structures.

In the next section, the measurement setup is described together with the adopted model, while a critical discussion of the results is presented in the subsequent section.

II. METHOD AND RESULTS

An Evatec CLUSTERLINE® 200 II multi-target co-sputtering deposition tool was used to deposit 250 nm ScAlN piezoelectric thin films on a blanket 100 nm-thick Platinum (Pt) layer. A 100 nm Pt top electrode was deposited and patterned by lift-off. Two geometric variables in the top electrodes of each test structure were varied, thereby generating a 2-dimensional matrix of devices: the radius a of the inner pad and the width w of the outer ring (see Fig. 1). The values of a and w were uniformly varied from 30 to 50 µm over five values and from 50 to 100 µm over six values, respectively, for a total of 30 test structures.

The experimental setup is shown in Fig. 2. A Form Factor Cascade ACP GSG-150 RF probe is used. After calibration, the complex reflection coefficient Γ (i.e. the S_{11} scattering parameter) has been measured by a Keysight N5221A Vector Network Analyzer (VNA), which is then converted into the impedance of the device under test (Z_{DUT}) via software.

The equivalent model of the DUT is shown in Fig. 3, and includes the capacitances between the bottom metal and both the inner metal pad C_{inner} and the outer metal ring C_{outer} in parallel with the resistances R_{inner} and R_{outer}, respectively, together with the resistance of the ring section R_{ring}. C_p can be neglected since the distance between the centers of the inner pad and the outer ring is always equal to the pitch of the used RF probe, i.e. 150 µm, while the dielectric thickness is equal to 250 nm. The total impedance of the test structure can be written as follows:

$$Z_{DUT} \approx Z_{inner} + R_{ring} + Z_{outer} \,, \qquad (1)$$

where $Z_{inner,outer}$ is the equivalent impedance of the parallel between $R_{inner,outer}$ and $C_{inner,outer}$.

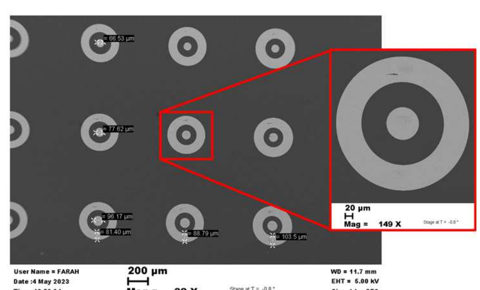

Fig. 1. SEM image of the fabricated matrix of DUTs.

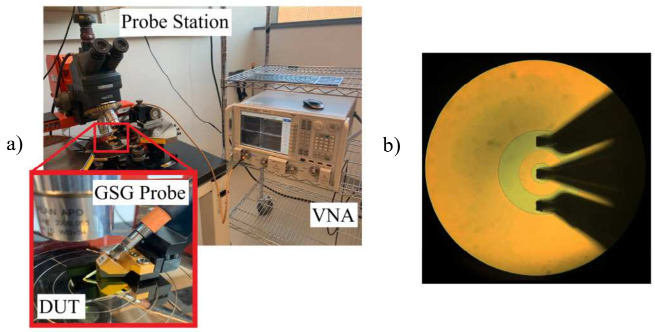

Fig. 2. a) S_{11} scattering parameter measurement setup; and b) DUT and landed GSG probe seen at the optical microscope.

The adopted method is a differential procedure based on the subtraction of the impedances measured from two test structures having the same outer ring (i.e. the ground), but different inner pad where the signal is applied. This approach removes the effect of parasitics due to the outer ground, since Z_{outer} is the same for both structures. This procedure was initially reported in [6], while in [7] accuracy limitations related to the same procedure are addressed. In both works, continuous grounds are used, while [8] applied the same technique to a test structure with a ground electrode consisting of an outer ring with a finite width. The following solution is presented, and it is adopted in this work to quantify the complex permittivity $\varepsilon_r = \varepsilon_r' - j\varepsilon_r''$ knowing that:

$$Z_{DUT\,1} - Z_{DUT\,2} = \frac{R_s}{2\pi} ln\left(\frac{a_2}{a_1}\right) + \frac{t}{j\omega\pi\varepsilon_0\varepsilon_r}\left(\frac{1}{a_1^2} - \frac{1}{a_2^2}\right), \quad (2)$$

where t is the thickness of the ScAlN layer and R_s the sheet resistance per square of the bottom metal layer.

Since ScAlN is piezoelectric, measurements show a thickness mode resonance within the frequency range of interest. To reduce its effects on the extraction, a Butterworth-Van Dyke (BVD) fitting was applied (see Fig. 4) [9]. The final results are obtained by de-embedding the fitted motional branch from the measured impedance. Fig. 5 shows the obtained dielectric constant ε_{33}, i.e. the real part ε_r' of the extracted complex permittivity, and loss tangent $tan\ \delta$, i.e. the ratio between its imaginary part ε_r'' and real one ε_r'.

III. Discussion

The thickness mode resonance fitting (see Fig. 4) is used to minimize its effect on the extracted quantities shown in Fig. 5. However, the discrepancy observed at low frequencies between the measured and the fitted resistance is likely attributable to a non-optimal calibration in that frequency range.

As expected from the results found in literature [10], the dielectric constant increases as the Sc doping concentration increases. While the dielectric constant seems to remain unchanged over the analyzed frequency range, the loss tangent increases linearly with frequency, an important trend to consider for the development of ScAlN RF piezoelectric resonators. The large fluctuations around the thickness mode resonance especially for the loss tangent are likely an artifact due to uncertainty in the fitting.

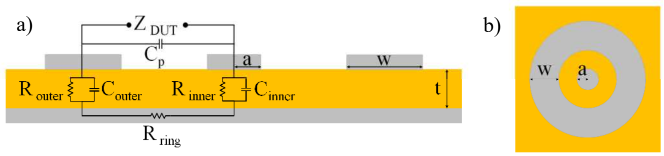

Fig. 3. a) Cross-section and lumped element equivalent electrical circuit of the DUT; and b) Top view of the DUT.

IV. Conclusions

In this paper, the complex permittivity of ScAlN thin films has been investigated for the Sc doping levels of 15% and 28%. The results reported in this work highlight and confirm its strong dependence on Sc doping concentration. The future work will focus on two further Sc doping levels, i.e. 0% and 36%, in order to provide a more complete view on the tunability of such properties. A wider frequency range will be also explored in order to investigate a possible dependence of the dielectric constant on the frequency, enabling the design of ScAlN RF piezoelectric resonators for 5G and 6G applications.

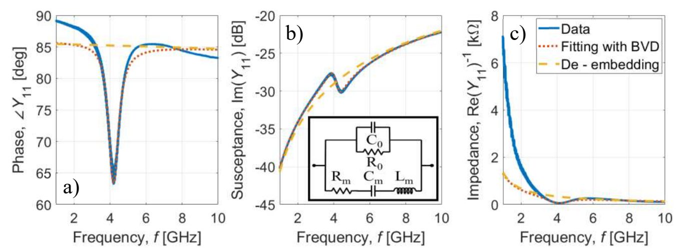

Fig. 4. a) Phase; b) Susceptance together with BVD model in the box; and c) Resistance. The solid blue lines represent the extracted data, while the dotted red lines and the dashed yellow ones the fitting with and without including the motional branch, respectively. The fictional trend of the resistance at low frequency has been separately fitted as a double exponential and de-embedded.

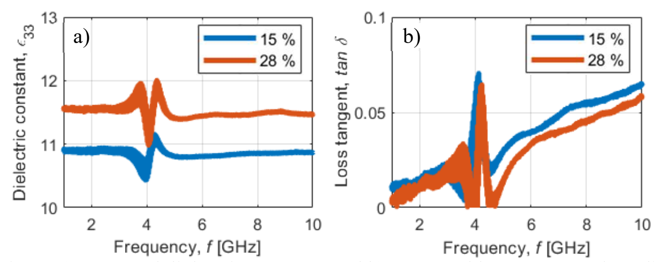

Fig. 5. a) Extracted dielectric constant; and b) Extracted loss tangent. The solid blue lines represent the average of the results for the DUTs with Sc doping of 15%, while the solid red lines the ones with Sc doping of 28%.

References

[1] Le, Xianhao, et al. "Piezoelectric MEMS—Evolution from sensing technology to diversified applications in the 5G/Internet of Things (IoT) era." *Journal of Micromechanics and Microengineering* 32.1 (2021): 014005.

[2] M. Pirro, et al. "Characterization of Dielectric and Piezoelectric Properties of Ferroelectric AlScN Thin Films," *2021 IEEE 34th International Conference on Micro Electro Mechanical Systems (MEMS)*, 2021, pp. 646-649.

[3] Zhu, Mingchi, Li Hua, and Fengfu Xiong. "First principles study on the structural, electronic, and optical properties of Sc-doped AlN." Russian Journal of Physical Chemistry A 88.4 (2014): 722-727.

[4] Krupka, Jerzy. "Frequency domain complex permittivity measurements at microwave frequencies." *Measurement Science and Technology* 17.6 (2006): R55.

[5] M. T. Khan, et al. "A brief review of measuring techniques for characterization of dielectric materials." *International Journal of Information Technology and Electrical Engineering* 1.1 (2012).

[6] Ma, Zhengxiang, et al. "RF measurement technique for characterizing thin dielectric films." *IEEE Transactions on electron devices* 45.8 (1998): 1811-1816.

[7] Rundqvist, Pär, et al. "Non-destructive microwave characterization of ferroelectric films on conductive substrates." *Integrated ferroelectrics* 60.1 (2004): 1-19.

[8] Sheng, S., et al. "Characterization of microwave dielectric properties of ferroelectric parallel plate varactors." *Journal of Physics D: Applied Physics* 42.1 (2008): 015501.

[9] H. Bhugra, and G. Piazza, eds. *Piezoelectric MEMS resonators*. New York, NY, USA: Springer International Publishing, 2017.

[10] Ambacher, O., et al. "Wurtzite ScAlN, InAlN, and GaAlN crystals, a comparison of structural, elastic, dielectric, and piezoelectric properties." *Journal of Applied Physics* 130.4 (2021): 045102.